

60.9, 59.0, 50.2, 44.4, 42.3, 38.5, 37.8, 37.5, 36.1, 36.0, 34.5, 33.7, 29.7, 28.6, 22.5, 19.3, 18.0, 17.6, 17.5, 14.1, 13.8, 12.8, 10.9; TLC R_f = 0.25 (5% MeOH/CH₂Cl₂). Exact mass: calcd for C₅₀H₈₁N₄O₁₅PNa, 1031.5333; found, 1031.5358 (FAB, *m*-nitrobenzyl alcohol, added NaI).

Acknowledgment. Support has been provided by the National Science Foundation and the National Institutes of Health. An NSF predoctoral fellowship to J.R.G. (1986-1989) is gratefully acknowledged. We are grateful to Professor N. Fusetani for kindly providing a sample of natural calyculin A. We thank Dr. Andrew Tyler of the Harvard Mass Spectrometry Facility for providing

mass spectra and acknowledge the NIH BRS Shared Instrumentation Grant Program 1 S10 RR0174801A1 and NSF (Grant CHE88-14019) for providing NMR facilities. Support from Upjohn and Merck are also acknowledged.

Supplementary Material Available: Full experimental details and complete analytical data for 6 → 7, 9 → 10, 11 → 12, 15 → 16, 22 → 23a, 29a → 29b, 29b → 30, 31 → 32, 40a → 40b, 49a → 49b, and 54a → 54b and the stereochemical proof of 48 (4 pages). Ordering information is given on any current masthead page.

Insertion of Transition Metals into the Phosphorus-Phosphorus Bond of 1,2-Dihydro-1,2-diphosphetes: Toward the Phosphorus Analogues of Metal Dithiolene Complexes

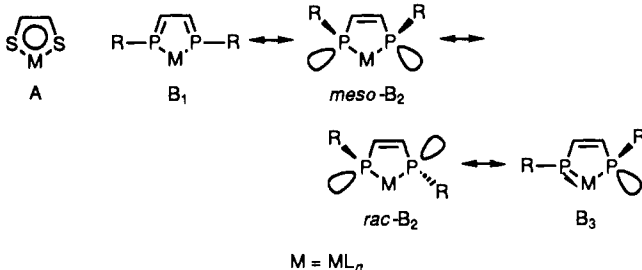
Gary Sillett, Louis Ricard, Carl Patois, and François Mathey*

Contribution from the Laboratoire de Chimie du Phosphore et des Métaux de Transition, UM13 CNRS, DCPH, Ecole Polytechnique, F-91128 Palaiseau Cedex, France.

Received December 23, 1991. Revised Manuscript Received August 6, 1992

Abstract: The insertion of NiL₂ (L = phosphine) into the P-P bond of 1,2,3,4-tetraphenyl-1,2-dihydro-1,2-diphosphete has been achieved via two methods. In the first, the P-P bond is initially cleaved with lithium and the derivatized dianion allowed to react with [NiCl₂L₂]. This yields primarily a nickeladiphospholene with a distorted square-planar geometry at the metal in which the chelating ligand acts as a (1 + 1) electron donor, and the metal is formally in the +2 oxidation state. The second route involves the direct insertion of a [NiL₂] fragment into the P-P bond at low temperature. In this case the results suggest the formation of a 1,4-diphosphadiene complex of nickel(0) in which the ligand acts as a (2 + 2) electron donor and the geometry at the metal is tetrahedral. Although both forms can be isolated for some coligands, only one form is observed in several cases and isomerization between the two forms has been observed in the other cases. The second route has also been transposed to platinum. The crystal structures of the Ni(Ph₂PCH₂CH₂PPH₂) and Pt(PPh₃)₂ complexes have been studied and a distortion from planarity observed in each case as shown by interplane LML/PMP angles of 38° and 57°, respectively. The phosphorus atoms are closer to planarity and the ring C=C bond lengths longer in the platinum complex than in the nickel. The platinum complex can be seen as lying halfway between a 1,4-diphospholene platinum(II) and a 1,4-diphosphadiene platinum(0) complex. This work suggests that with an adequate choice of coligand and substitution pattern it would be possible to achieve an electronic delocalization similar to that observed in metal-dithiolenes.

The metal dithiolene structure (A) is characterized by the indeterminate nature of the metal oxidation state. This kind of metallacycle finds numerous applications as redox catalysts, dyes, organic conductors, etc.¹ We thought it would be interesting to prepare the analogous metalladiphospholenes (B).



To the best of our knowledge no such potentially delocalized metallacycle has been structurally characterized in the literature although two iridadiphospholenes have been identified in solution

by NMR spectroscopy.² There is an obvious correlation between the oxidation state of the metal and the structure of the ring in a metalladiphospholene. The mesomeric formula (B₁), where the metal is in the 0 oxidation state, corresponds to (2 + 2) electron donation from the chelating ligand, with planar phosphorus atoms, two P=C double bonds, and a C-C single bond. Conversely, the mesomeric formula (B₂), where the metal is in the +2 oxidation state, corresponds to (1 + 1) electron donation from the chelating ligand, with pyramidal phosphorus atoms, two intracyclic P-C single bonds, and a C=C double bond. The presence of two chiral phosphorus atoms in this latter case implies two possible diastereoisomers (meso and racemic). Finally the mesomeric formula (B₃), with the metal still in the +2 oxidation state, corresponds to (3 + 1) electron donation from the chelating ligand, with one pyramidal and one planar phosphorus atom, one single and one double M-P bond, but two P-C single bonds and a C=C double bond as in (B₂).

Situations corresponding to *meso*-B₂, *rac*-B₂, and B₃ have been identified by Lappert and co-workers³ in the study of benzo analogues with zirconium, tin, or boron as the metal. A priori, benzo annellation has an adverse effect on the electronic delo-

(1) For recent reviews on metal dithiolenes see: Mueller-Westerhoff, U. T.; Vance, B. *Dithiolenes and Related Species*. In *Comprehensive Coordination Chemistry*; Wilkinson, G., Gillard, R. D., McCleverty, J. A., Eds.; Pergamon: Oxford, 1987; Vol. 2, pp 595-631. Mueller-Westerhoff, U. T.; Vance, B.; Yoon, D. I. *Tetrahedron* 1991, 47, 909.

(2) Phillips, I. G.; Ball, R. G.; Cavell, R. G. *Inorg. Chem.* 1988, 27, 2269.

(3) Bohra, R.; Hitchcock, P. B.; Lappert, M. F.; Leung, W.-P. *Chem. Soc., Chem. Commun.* 1989, 728.

Table I. ^{31}P NMR Data for Nickeladiphospholenes $[\text{Ni}(\text{C}_2\text{Ph}_4\text{P}_2)(\text{L})_2]$ via the $[\text{NiCl}_2(\text{L})_2]$ Route

L	complex	$\delta^{31}\text{P}$ ($\text{C}_2\text{Ph}_4\text{P}_2$)	δP (L)	spin system	$\sum J_{\text{AX}} + J_{\text{AX}'}$ or $^2J_{\text{PNiP}}$, Hz
$1/2\text{DPPE}^a$	4	+89	+52	AA'XX'	$\sum = 88$
PPh_3	5	+131	+35	A_2X_2	$^2J = 42$
$\text{PPh}(\text{CH}_2\text{Ph})_2$	6a	+89	+51	AA'XX'	$\sum = 97$
PMc_2Ph	7	+106	-3	A_2X_2	$^2J = 51$
PEt_3	8a	+90	+52	AA'XX'	$\sum = 97$
P^nBu_3	9a	+89	+52	AA'XX'	$\sum = 97$

^a DPPE = $\text{Ph}_2\text{PCH}_2\text{CH}_2\text{PPh}_2$.**Table II.** ^{31}P NMR Data for Nickeladiphospholenes $[\text{Ni}(\text{C}_2\text{Ph}_4\text{P}_2)(\text{L})_2]$ via the $[\text{Ni}(\text{L})_2]$ Route

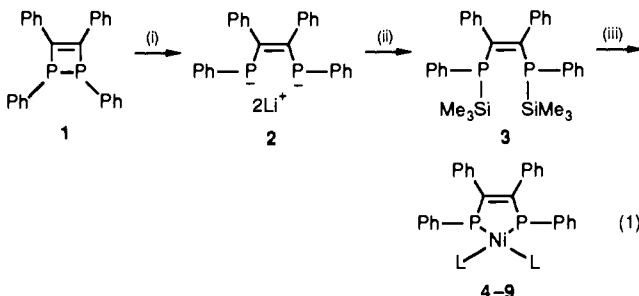
L	complex	$\delta^{31}\text{P}$ ($\text{C}_2\text{Ph}_4\text{P}_2$)	δP (L)	spin system	$\sum J_{\text{AX}} + J_{\text{AX}'}$ or $^2J_{\text{PNiP}}$, Hz
$1/2\text{DPPE}^a$	4	+89	+52	AA'XX'	$\sum = 88$
$\text{PPh}(\text{CH}_2\text{Ph})_2$	6b	+103	+24	A_2X_2	$^2J = 49$
PMc_2Ph	7	+106	-3	A_2X_2	$^2J = 51$
PEt_3	8b	+113	+19	A_2X_2	$^2J = 48$
P^nBu_3	9b	+114	+11	A_2X_2	$^2J = 49$
$1/2\text{DPPP}^b$	10	+113	+15	A_2X_2	$^2J = 44$

^a DPPE = $\text{Ph}_2\text{P}(\text{CH}_2)_2\text{PPh}_2$. ^b DPPP = $\text{Ph}_2\text{P}(\text{CH}_2)_3\text{PPh}_2$.

calization within the metalladiphospholene ring and its suppression could shift the overall structure of the ring toward the B_1 limit. We chose therefore to investigate the interaction of the readily available 1,2,3,4-tetraphenyl-1,2-dihydro-1,2-diphosphete (**1**)⁴ with NiL_2 and PtL_2 centers (L = phosphine). With these systems the structure (tetrahedral or square-planar) and the para- or diamagnetism of the complex provide additional information on the oxidation state of the metal.

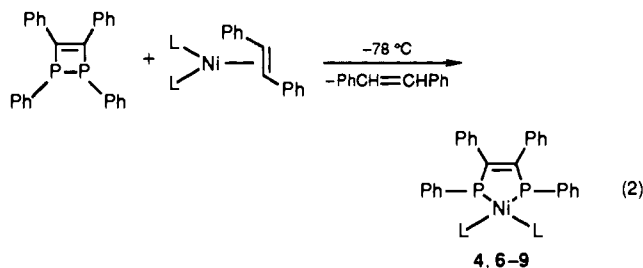
Results and Discussion

With nickel as the metal we have chosen two synthetic strategies. In the first, the P-P bond of **1** is cleaved by lithium in THF to give the corresponding dianion **2**.⁵ The direct reaction of **2** with $[\text{NiCl}_2(\text{PR}_3)_2]$ reforms the starting heterocycle via a redox process. We avoided this by preparing the silyl derivative **3** which cleanly reacts with $[\text{NiCl}_2(\text{PR}_3)_2]$ to yield the expected nickeladiphospholenes **4-9** (eq 1). These nickeladiphospholenes

(i) Li/THF; (ii) SiClMe_3 ; (iii) $[\text{NiCl}_2\text{L}_2]$

were characterized by ^{31}P NMR spectroscopy, and the corresponding results are collected in Table I. In the second route, 14-electron zero-valent NiL_2 species were inserted directly into the P-P bond of the 1,2-dihydro-1,2-diphosphete (eq 2). The results of these experiments are collected in Table II.

All of these compounds are diamagnetic but two main types of spectrum are observed (Figure 1), i.e., an [AA'XX'] and an $[\text{A}_2\text{X}_2]$ spin system, where for a given phosphine, L, the chemical shift values for A and X are significantly different in each type of spectrum. Variable-temperature experiments down to -80°C show no variation of these spectra with the exception of **4** which is fluxional in solution, exhibiting a degenerate [AA'XX'] spectrum at higher temperatures, a normal [AA'XX'] spectrum at lower



temperatures, invariant lines, and no change in chemical shift values. It is important to note that in some cases (L = $1/2\text{DPPE}$, PMc_2Ph , PPh_3) both routes yield the same product, and in others the $[\text{NiCl}_2(\text{PR}_3)_2]$ route yields the [AA'XX'] product whereas the $[\text{NiL}_2]$ route yields the $[\text{A}_2\text{X}_2]$ product. In all cases except **4**, the [AA'XX'] slowly transforms into the corresponding $[\text{A}_2\text{X}_2]$ products at room temperature. A typical spectrum showing this transformation for **8** is shown in Figure 1. Besides **8a** and **8b**, an additional transient product **8c** appears at the beginning of the transformation of **8a** and disappears with it, leaving pure **8b** at the end of the reaction. Product **8c** displays a first-order [AJMX] spectrum with δ_A 89.8, δ_J 85.7, δ_M 58.4, and δ_X 43.4 and $J_{\text{AJ}} = 4.7$ Hz, $J_{\text{AM}} = 63$ Hz, $J_{\text{AX}} = 20.2$ Hz, $J_{\text{JM}} = 26$ Hz, $J_{\text{JX}} = 67.2$ Hz, and $J_{\text{MX}} = 10.7$ Hz.

Our interpretation of these results is as follows. The $[\text{NiCl}_2(\text{PR}_3)_2]$ route yields primarily the [AA'XX'] product and the $[\text{NiL}_2]$ route yields primarily the $[\text{A}_2\text{X}_2]$ product. The transformation of the [AA'XX'] into the $[\text{A}_2\text{X}_2]$ product proceeds via the [AJMX] species. These three systems represent isomers of the same molecule. The fact that with certain phosphines as coligands we separately observe each distinct isomer suggests that the activation barriers for the interconversions between the three are significant. However, the fact that we are able to observe a transformation between them in most cases at room temperature indicates that these barriers are nevertheless accessible, and that the energies of the three isomers are similar.

Whereas [AA'XX'] and [AJMX] spin systems could correspond to almost any conceivable situation, the $[\text{A}_2\text{X}_2]$ spin system puts severe constraints on the structures of the corresponding compounds. Indeed, coincidental degeneracy ($J_{\text{AX}} = J_{\text{AX}'}$) of a [AA'XX'] system is not conceivable for a whole series of products. In this latter case, the nickel coordination sphere must have tetrahedral symmetry and the two sides of the nickeladiphospholene ring must be equivalent. Hence the *meso*- B_2 and B_3 structures can be excluded and only structures B_1 and *rac*- B_2 are acceptable. However, the diamagnetism of these tetrahedral complexes implies the filling of the three degenerate d_{xy} , d_{yz} , and d_{zx} orbitals of the metal and thus that the 1,2-dihydro-1,2-diphosphete must act as a four-electron ligand. Therefore, the only satisfactory explanation is that the $[\text{A}_2\text{X}_2]$ systems correspond to tetrahedral 1,4-diphosphadiene complexes of zero-valent nickel, structure B_1 . This hypothesis also accounts for the tendency toward lower fields for the $\text{P}(\text{A})$ resonance when comparing the $[\text{A}_2\text{X}_2]$ spectra with the [AA'XX'] spectra.

From a chemical standpoint, it is easy to rationalize why the $[\text{A}_2\text{X}_2]\text{Ni}^0$ complexes are obtained via the NiL_2 route. Both theoretical calculations⁶ and experimental data⁷ have shown that there is a potential equilibrium between 1,2-dihydro-1,2-diphosphetes and 1,4-diphosphadienes, although this equilibrium is completely shifted toward the cyclic structure at room temperature in most cases. The insertion of $[\text{NiL}_2]$ into the P-P bond can be viewed, in fact, as a trapping of the diphosphadiene isomer with displacement of the equilibrium toward the open form. A more or less related reaction has been described by Nixon and his group⁸ between $[\text{PtL}_2]$ and a 1,2-dihydrophosphete ring. The platinum complex traps the 1-phosphadiene isomer at room temperature.

(4) Ricard, L.; Maigrot, N.; Charrier, C.; Mathey, F. *Angew. Chem., Int. Ed. Engl.* 1987, 26, 548.(5) Charrier, C.; Guilhem, J.; Mathey, F. *J. Org. Chem.* 1981, 46, 3.(6) Bachrach, S. M.; Liu, M. *J. Org. Chem.* 1992, 57, 2040.(7) Maigrot, N.; Charrier, C.; Ricard, L.; Mathey, F. *Polyhedron* 1990, 9, 1363.(8) Ajulu, F. A.; Al-Juaid, S. S.; Carmichael, D.; Hitchcock, P. B.; Meidine, M. F.; Nixon, J. F.; Mathey, F.; Tran-Huy, N. H. *J. Organomet. Chem.* 1991, 406, C20.

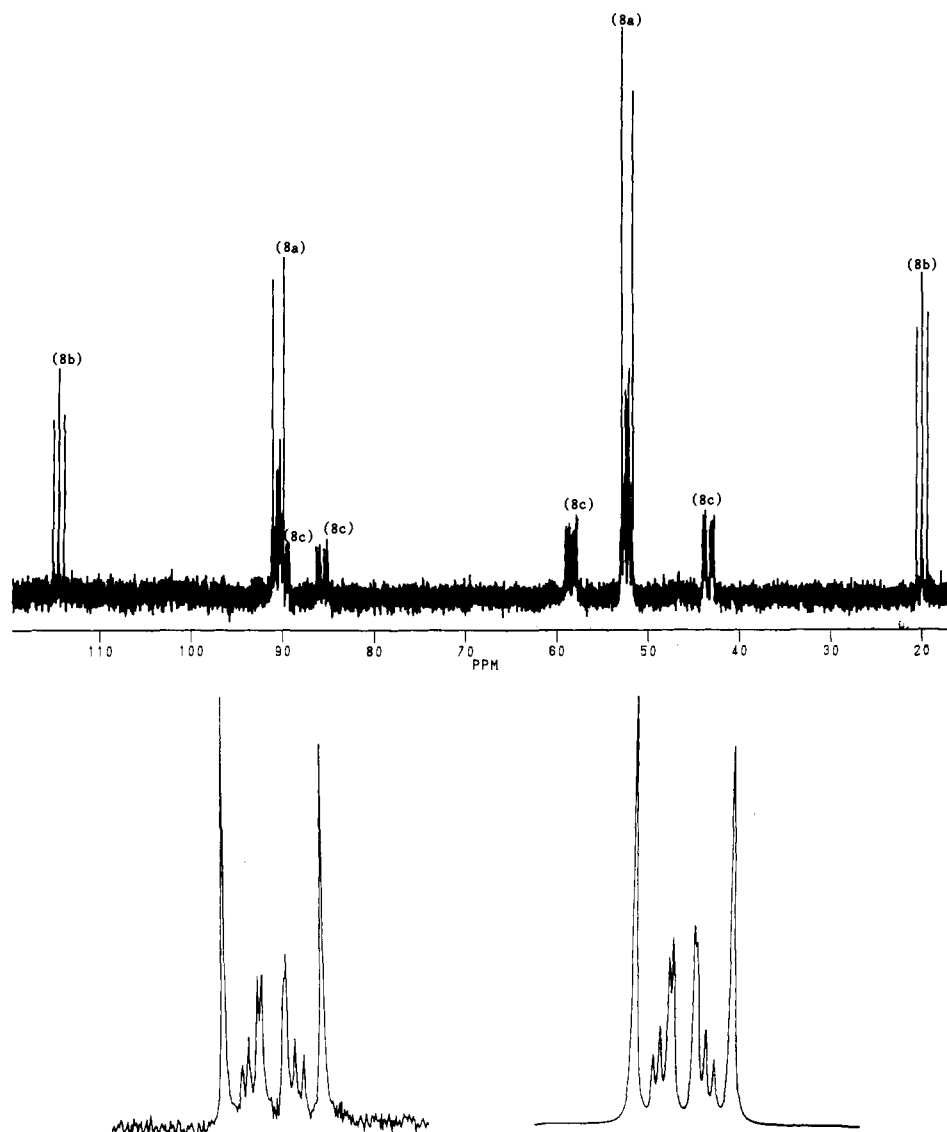


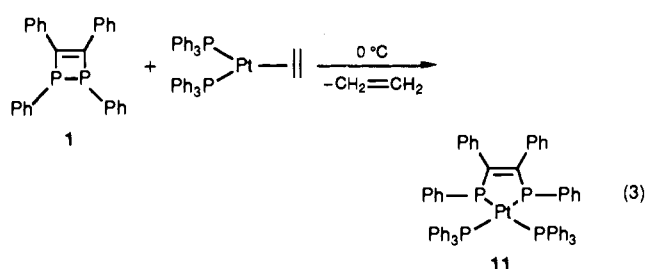
Figure 1. (a, top) 81.01-MHz ³¹P{¹H} NMR spectrum of a toluene solution showing the conversion of **8a** into **8b**. The transient product **8c** disappears together with **8a** at the end of the reaction. (b, bottom) Simulation of the low-frequency component of the [AA'XX'] spectrum of **8a**: $\delta P_A = \delta P_{A'} = 90.5$ ppm; $\delta P_X = \delta P_{X'} = 52$ ppm; $J_{AA'} = 14.17$ Hz; $J_{AX} = J_{A'X'} = 30.61$ Hz; $J_{AX} = J_{A'X} = 66.38$ Hz; $J_{XX'} = 5.46$ Hz.

In order to test our hypothesis we decided to investigate the X-ray crystal structures of several compounds in this family. We were first able to obtain satisfactory crystals of complex **4**, and its structure is depicted in Figure 2.

Complex **4** can be described as a distorted square-planar nickel complex with an interplane ($P_1NiP_4/P_{29}NiP_{32}$) angle of almost 38°. The nickeladiphospholene ring is practically planar, C₂ being 0.20 Å outside of the $P_1NiP_4C_3$ plane, causing a $P_1C_2C_3P_4$ torsion angle of 14°, the C=C double bond within the ring appears to be well localized at 1.354 (6) Å, the P—C bonds have single bond character (1.806 Å mean), and the ring phosphorus atoms are pyramidal ($\sum P_1 = 330^\circ$ and $\sum P_4 = 327^\circ$). Thus the best formulation for **4** is the *rac*-B₂ type. From another standpoint, it is not surprising to find that the chelating DPPE freezes the transformation of the *rac*-B₂ into the B₁ structure. Indeed, this transformation induces a substantial widening of the LNiL angle which is disfavored by the chelating ligand. On the contrary, it is not surprising to find that bulky coligands such as PPh₃ favor the [A₂X₂] tetrahedral structure.

In spite of considerable effort, we were unable to grow satisfactory crystals of one of the [A₂X₂] species and so to obtain a better structural basis for our hypothesis we decided to investigate an analogous platinum complex. It is, of course, difficult to transpose the [NiCl₂(PR₃)₂] route since the redox reaction between the dianion **2** and a platinum(II) center is even easier than with

nickel, and the facile oxidative addition of SiClMe₃ to platinum(II) prevents the application of the modified route shown in eq 2. Thus we chose to insert a [PtL₂] fragment into the P—P bond of **1** as shown in eq 3.



The [AA'XX'] system in the ³¹P{¹H} NMR spectrum showed that **11** is not tetrahedral, but as we were able to grow satisfactory crystals we decided to study its structure (Figure 3). The first striking result is that the interplane angle ($P_1PtP_4/P_{29}PtP_{48}$) is almost 57° and thus the structure of **11** is much closer to the tetrahedral limit than is that of **4** (Figure 4). As in **4**, although $P_1PtP_4C_3$ is planar, C₂ is again displaced from this plane (0.26 Å), causing a $P_1C_2C_3P_4$ torsion angle of 19°.

According to our previous reasoning, the substructure of the chelate dihydrodiphosphete unit should be closer to the B₁ limit.

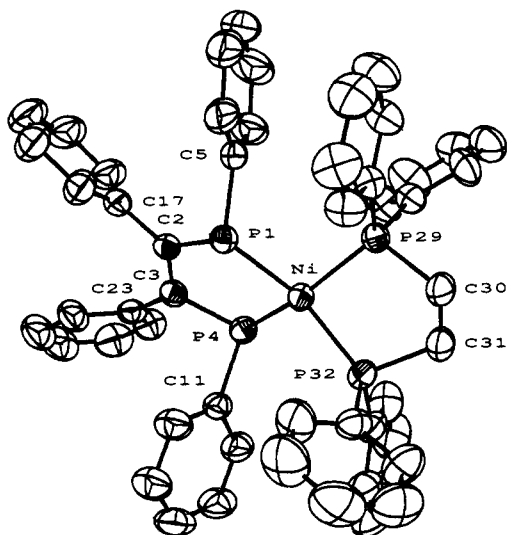


Figure 2. Structure of **4** in the crystal. Ellipsoids are scaled to enclose 50% of the electron density. Hydrogen atoms are omitted for clarity. Important bond lengths (Å) and angles (deg): Ni–P(1) 2.164 (1), Ni–P(4) 2.173 (1), Ni–P(29) 2.186 (1), Ni–P(32) 2.183 (1), P(1)–C(2) 1.803 (3), C(2)–C(3) 1.354 (6), C(3)–P(4) 1.808 (4), P(1)–Ni–P(4) 85.22 (4), P(1)–Ni–P(29) 98.20 (4), P(1)–Ni–P(32) 155.38 (5), P(4)–Ni–P(29) 153.27 (5), P(4)–Ni–P(32) 99.59 (4), P(29)–Ni–P(32) 88.30 (4), Ni–P(1)–C(2) 110.9 (1), Ni–P(1)–C(5) 119.4 (1), C(2)–P(1)–C(5) 99.5 (2), Ni–P(4)–C(3) 111.0 (1), Ni–P(4)–C(11) 116.5 (1), C(3)–P(4)–C(11) 99.2 (2).

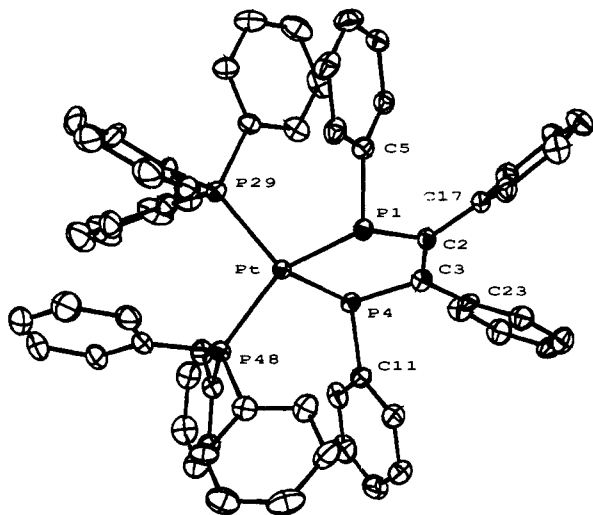


Figure 3. Structure of **11** in the crystal. Ellipsoids are scaled to enclose 50% of the electron density. Hydrogen atoms are omitted for clarity. Important bond lengths (Å) and angles (deg): Pt–P(1) 2.288 (2), Pt–P(4) 2.282 (1), Pt–P(29) 2.312 (2), Pt–P(48) 2.329 (1), P(1)–C(2) 1.797 (6), C(2)–C(3) 1.376 (9), C(3)–P(4) 1.799 (6), P(1)–Pt–P(4) 82.67 (6), P(1)–Pt–P(29) 102.11 (6), P(1)–Pt–P(48) 140.95 (6), P(4)–Pt–P(29) 136.35 (6), P(4)–Pt–P(48) 98.34 (5), P(29)–Pt–P(48) 103.39 (6), Pt–P(1)–C(2) 110.0 (2), Pt–P(1)–C(5) 119.6 (2), C(2)–P(1)–C(5) 105.9 (3), Pt–P(4)–C(3) 111.5 (2), Pt–P(4)–C(11) 123.3 (2), C(3)–P(4)–C(11) 102.5 (3).

This is indeed the case as the two phosphorus atoms are more planar than in **4**, ($\Sigma = 336^\circ$ and 337°). If the intracyclic P–C bonds are only marginally shorter than in **4** at 1.798 Å (mean), the C=C ring bond is however significantly longer at 1.376 (9) Å. These data are all the more meaningful when compared with those for a well-localized platinaphospholene ring⁸ where the intracyclic P–C bond length is 1.832 (5) Å and the ring C=C bond is 1.329 (9) Å. It is indeed quite clear that we are close to the B₁ limit. As in **4** the M–P(dihydrophosphate) bonds in **11** are shorter than the M–P(phosphine) bonds at 2.288 (2) and 2.282 (1) Å compared to 2.312 (2) and 2.329 (1) Å. It is interesting to note that the Pt–P ring bond in the previously mentioned platinaphospholene is longer than those of **11** at 2.326

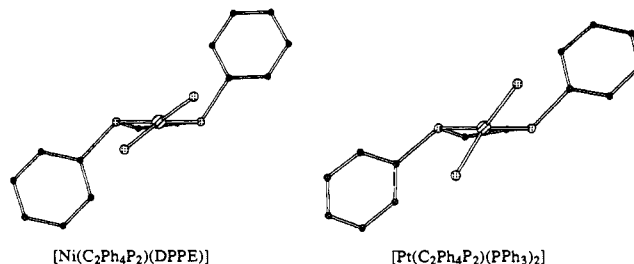


Figure 4. Representations of the relationship between the $(R_3P)_2M$ plane and the $(C_2Ph_4P_2)M$ plane for **4** and **11**.

(2) Å, which is in line with the assumption that in **11** the chelating dihydrodiphosphate donates more than $(1 + 1)$ electrons to the metal center.

To summarize, we can state that nickeladiphospholenes exist in mainly two stable forms, one corresponding to a 1,4-diphosphadiene–nickel(0) complex with a tetrahedral structure where the ligand acts as a $(2 + 2)$ electron donor (B₁) and a second corresponding more closely to the nickeladiphospholene formulation where the ligand acts as a $(1 + 1)$ electron donor, the *rac*-B₂ structure, and where the nickel has a more or less square-planar geometry. In many cases, the *rac*-B₂ transforms at room temperature into the B₁ form via a third transient species of low symmetry and of unknown structure. The only structurally characterized platinadiphospholene is half-way between these two structures. Clearly, with these systems we are close to the electronic delocalization which is responsible for the special physical and catalytic properties of the metal dithiolene complexes.

Experimental Section

General Data. All reactions were performed under an argon atmosphere using standard Schlenk and vacuum-line techniques. Solvents were purified and dried using standard methods and freshly distilled prior to use. NMR spectra were recorded on Bruker AC200SY (¹H, 200.1; ³¹P, 80.1; and ¹³C, 50.3 MHz) and WP80 (³¹P, 32.4 MHz) spectrometers. *J* values are reported in hertz. Chemical shifts are quoted in parts per million with positive values downfield from internal TMS (¹³C and ¹H) and external 85% H₃PO₄ (³¹P) references. Mass spectra were obtained at 70 eV using a Shimadzu GC-MS QP 1000 instrument by the direct inlet method. All of the compounds are air and moisture sensitive.

X-ray Structure Determinations. Data were collected on an Enraf-Nonius CAD4 diffractometer using Mo K α radiation ($\lambda = 0.71073$ Å) and a graphite monochromator. The crystal structures were solved and refined using the Enraf-Nonius SDP package. The hydrogen atoms were included as fixed contributions in the final stages of least-squares refinement while using anisotropic temperature factors for all other atoms. A non-Poisson weighting scheme was applied in both cases.

Crystals of **4**, C₅₂H₄₄NiP₄^{1/2}C₇H₈, were grown at room temperature from a hexane–toluene (4:1) solution of the compound. The complex crystallizes in space group $P\bar{1}$, $a = 10.151$ (1) Å, $b = 10.544$ (1) Å, $c = 23.570$ (2) Å, $\alpha = 94.81$ (1) $^\circ$, $\beta = 98.58$ (1) $^\circ$, $\gamma = 106.85$ (1) $^\circ$; $V = 2365.85$ (93) Å³; $Z = 2$; $d(\text{calc}) = 1.260$ g/cm³; $\mu = 5.8$ cm⁻¹; $F(000) = 952$; temperature for data collection = 20 ± 1 °C. A total of 8307 unique reflexions were recorded in the range $2^\circ \geq 2\theta \geq 50.0^\circ$ of which 3712 were considered as unobserved ($F^2 < 3.0\sigma(F^2)$), leaving 4595 for solution and refinement. Direct methods yielded a solution for 20 atoms, including nickel and phosphorus. The final agreement factors were $R = 0.039$, $R_w = 0.054$, and GOF = 1.04 with $p = 0.08$.

Complex **11**, C₆₂H₅₀P₄PtC₇H₈, was crystallized at room temperature from a toluene solution. The compound belongs to space group $P2_12_12_1$, $a = 12.592$ (1) Å, $b = 19.291$ (2) Å, $c = 22.483$ (2) Å; $V = 5461.23$ (1.48) Å³; $Z = 4$; $d(\text{calc}) = 1.469$ g/cm³; $\mu = 27.6$ cm⁻¹; $F(000) = 2440$; temperature for data collection = -150 ± 0.5 °C. A total of 8142 unique reflexions were recorded in the range $2^\circ \geq 2\theta \geq 60.0^\circ$ of which 6124 were used for solution and refinement. The initial model was obtained from a Patterson map. The final agreement factors were $R = 0.029$, $R_w = 0.038$, and GOF = 1.05 with $p = 0.05$. The *R* factors of the enan-

tiomeric structure were respectively equal to 0.060 and 0.081, GOF = 2.27.

Synthesis of $C_2Ph_4P_2Li_2$ (2). The dianion was synthesized by treatment of 1,2,3,4-tetraphenyl-1,2-dihydro-1,2-diphosphete (1) with 2 equiv of lithium according to the method outlined in ref 5. The product was used as a solution in THF without further purification.

Synthesis of $C_2Ph_4P_2(SiMe_3)_2$ (3). A solution of 2 (5 mmol) in 25 mL of THF was cooled to $-78^\circ C$ and chlorotrimethylsilane (1.3 mL, 1.1 g, 10 mmol) added dropwise by syringe. The mixture was allowed to stir at $-78^\circ C$ until the color had faded to orange-yellow, and the $^{31}P\{^1H\}$ NMR spectrum indicated complete formation of the silylated product. The mixture was allowed to attain ambient temperature and the THF removed in vacuo to give a yellow oil which was extracted into 50 mL of a (5:1) hexane-toluene mixture. The resulting suspension was rapidly filtered through Celite and the solvent removed in vacuo from the filtrate to give 3 as a yellow oil which was characterized by ^{31}P NMR spectroscopy and used, without further purification owing to its sensitivity to moisture and air, as a solution (0.1 M) in toluene. $^{31}P\{^1H\}$ (THF): $\delta^{31}P$ -45 ppm.

Synthesis of $[Ni(\eta^2-PhCH=CHPh)(PR_3)_2]$. $[NiCl_2(PR_3)_2]$ (1 mmol) was suspended in a toluene solution of *trans*-stilbene (200 mg, 1.1 mmol, in 30 mL) and cooled to $0^\circ C$. SuperHydride (2 mL, 2 mmol) was added dropwise by syringe and the mixture allowed to stir at $0^\circ C$ for 5 min. During this time the suspended nickel starting complex dissolved, the color changed from deep red to a yellow-brown, and a gas was evolved. The mixture was allowed to attain ambient temperature (5 min), and the formation of the η^2 -nickel(0) complex was verified by ^{31}P NMR spectroscopy. The mixture was subsequently cooled to $-78^\circ C$ and used immediately. $^{31}P\{^1H\}$: δP (THF) +42 (DPPE), +22 ($PPh(CH_2Ph)_2$), +17 (PEt_3), +9 (DPPP), +8 (P^tBu_3), -3 (PMe_2Ph).

Synthesis of $[Ni(C_2Ph_4P_2)(PR_3)_2]$. (a) $[NiCl_2(PR_3)_2]$ (2 mmol) was suspended in toluene (30 mL) and cooled to $0^\circ C$. 3 (2 mmol) was added dropwise as a toluene solution (20 mL) causing the dissolution of the suspended nickel(II) complex. The solvent was removed in vacuo and the residue washed with cold hexane (3×5 mL at $-78^\circ C$). The residue

was dissolved in a minimum of toluene and the complex precipitated with hexane ($PR_3 = \frac{1}{2}DPPE, PPh(CH_2Ph)_2$). $^{31}P\{^1H\}$ NMR (toluene): (4) +89, +52 ($AA'XX'$, $\sum J_{AX} + J_{AX'} = 88$); (5) +131, +35 (A_2X_2 , $^2J_{PNIP} = 42$); (6a) +89, +51 ($AA'XX'$, $\sum J_{AX} + J_{AX'} = 98$); (7) +106, -3 (A_2X_2 , $^2J_{PNIP} = 51$); (8a) +90, +52 ($AA'XX'$, $\sum J_{AX} + J_{AX'} = 94$); (9a) +89, +52 ($AA'XX'$, $\sum J_{AX} + J_{AX'} = 98$). $^{13}C\{^1H\}$ NMR (CD_2Cl_2): (4) 1.3 (m, CH_2), 155.2 (d, $^1J_{PC} = 47$ Hz, $=C-P$). 1H NMR (CD_2Cl_2): (4) 2.11 (4 H, b, CH_2), 6.9-7.7 (40 H, m, Ph). Mass spectra (EI, 70 eV): (4) *m/z* 849 ($M^+ - H$, 10%), 398 ($Ph_2PCH_2CH_2PPh_2^+$, 87%), 394 ($C_2Ph_4P_2^+$, 100%).

(b) To a toluene solution of $[Ni(\eta^2-PhCH=CHPh)(PR_3)_2]$ (1 mmol in 30 mL) cooled to $-78^\circ C$ was rapidly added a toluene solution of $C_2Ph_4P_2$ (395 mg, 1 mmol). The mixture was stirred for 1 min and then examined by ^{31}P NMR spectroscopy. $^{31}P\{^1H\}$ NMR (toluene): (4) +89, +52 ($AA'XX'$, $\sum J_{AX} + J_{AX'} = 88$); (6b) +103, +24 (A_2X_2 , $^2J_{PNIP} = 49$); (7) +106, -3 (A_2X_2 , $^2J_{PNIP} = 51$); (8b) +113, +19 (A_2X_2 , $^2J_{PNIP} = 48$); (9b) +114, +11 (A_2X_2 , $^2J_{PNIP} = 49$). $^{13}C\{^1H\}$ NMR (CD_2Cl_2): (4) 1.3 (m, CH_2), 155.2 (d, $^1J_{PC} = 47$ Hz, $=C-P$). 1H NMR (CD_2Cl_2): (4) 2.11 (4 H, b, CH_2), 6.9-7.7 (40 H, m, Ph).

Synthesis of $[Pt(C_2H_4)(PPh_3)_2]$ (148 mg, 0.2 mmol) and 1 (80 mg, 0.2 mmol) were separately dissolved in 3 mL of toluene and cooled to $0^\circ C$. The solution and the platinum(0) complex was added to the solution of 1 by transfer wire, a reaction occurring immediately with the evolution of a gas to give a deep red solution. The solvent was removed in vacuo and the residue washed with hexane (2×5 mL) to give an orange-red solid. $^{31}P\{^1H\}$ NMR (toluene): δP ($C_2Ph_4P_2$) +77 ($^1J_{PIP} = 1512$); δP (PPh_3) +29 ($^1J_{PIP} = 3122$; $\sum J_{AX} + J_{AX'} = 132$).

Supplementary Material Available: Tables of crystallographic data, positional and displacement parameters, and bond distances and angles (25 pages); tables of observed and calculated structure factors (58 pages). Ordering information is given on any current masthead page.

Electrochemical Synthesis of Ceramic Materials. 2. Synthesis of AlN and an AlN Polymer Precursor: Chemistry and Materials Characterization

Travis Wade, Jongman Park, Ernest Gene Garza, Claudia B. Ross, Douglas M. Smith, and Richard M. Crooks*

Contribution from the UNM/NSF Center for Micro-Engineered Ceramics, University of New Mexico, Albuquerque, New Mexico 87131. Received June 26, 1992

Abstract: A simple electrochemical method for the preparation of AlN and other metal nitride ceramic precursors is described. Constant-current electrolysis in a cell containing a NH_4Br/NH_3 electrolyte solution and Al electrodes yields a solid mixture consisting primarily of $Al(NH_3)_6Br_3$ and $[Al(NH_2)(NH)]_n$ after excess NH_3 is removed. Calcination of this mixture above $600^\circ C$ in flowing NH_3 results in elimination of $Al(NH_3)_6Br_3$ and conversion of the AlN polymer precursor, $[Al(NH_2)(NH)]_n$, to high surface area AlN powder containing low levels of oxygen and carbon impurities. In this report, some electrochemical aspects of the AlN polymer precursor synthesis and processing are discussed. Characterization of the AlN powder before and after sintering is also discussed.

Introduction

In this paper, we discuss a new electrochemical method for synthesizing an inorganic AlN polymer precursor. Metal nitride ceramics represent an important area of research at the present time, because they often have superior electronic, thermal, or mechanical characteristics compared to those of the corresponding oxides. For example, compared to Al_2O_3 , AlN has much higher thermal conductivity, a better thermal expansion match to Si, lower electrical conductivity, comparable mechanical strength, and optical properties that are suitable for optoelectronics ap-

plications in some cases.¹⁻³ However, metal nitride ceramics have not as yet found widespread commercial applications, because they are generally more challenging and costly to synthesize and process than oxides. The purpose of this paper is to introduce a new synthetic method that yields an AlN polymer precursor, which can be calcined at relatively low temperature to yield pure-metal or mixed-metal nitride ceramics with desirable morphological and compositional characteristics. We have chosen to focus this paper

- (1) Sheppard, L. M. *Am. Ceram. Soc. Bull.* 1990, 69, 1801.
- (2) Kuramoto, N.; Taniguchi, H. *J. Mater. Sci. Lett.* 1984, 3, 471.
- (3) Marchant, D. D.; Nemecek, T. E. *Adv. Ceram.* 1989, 26, 19.

* Author to whom correspondence should be addressed.